

Supporting Information for

**Hierarchical Core/Shell Janus-type  $\alpha$ -Fe<sub>2</sub>O<sub>3</sub>/PEDOT**

**Nanoparticles for High Performance Flexible Energy Storage  
Devices**

*Jin Wook Park, Wonjoo Na and Jyongsik Jang\**

[\*] Prof. J. Jang, J. W. Park, W. Na  
School of Chemical and Biological Engineering, Seoul National University, Seoul 151-742,  
Korea  
E-mail: [jsjang@plaza.snu.ac.kr](mailto:jsjang@plaza.snu.ac.kr)

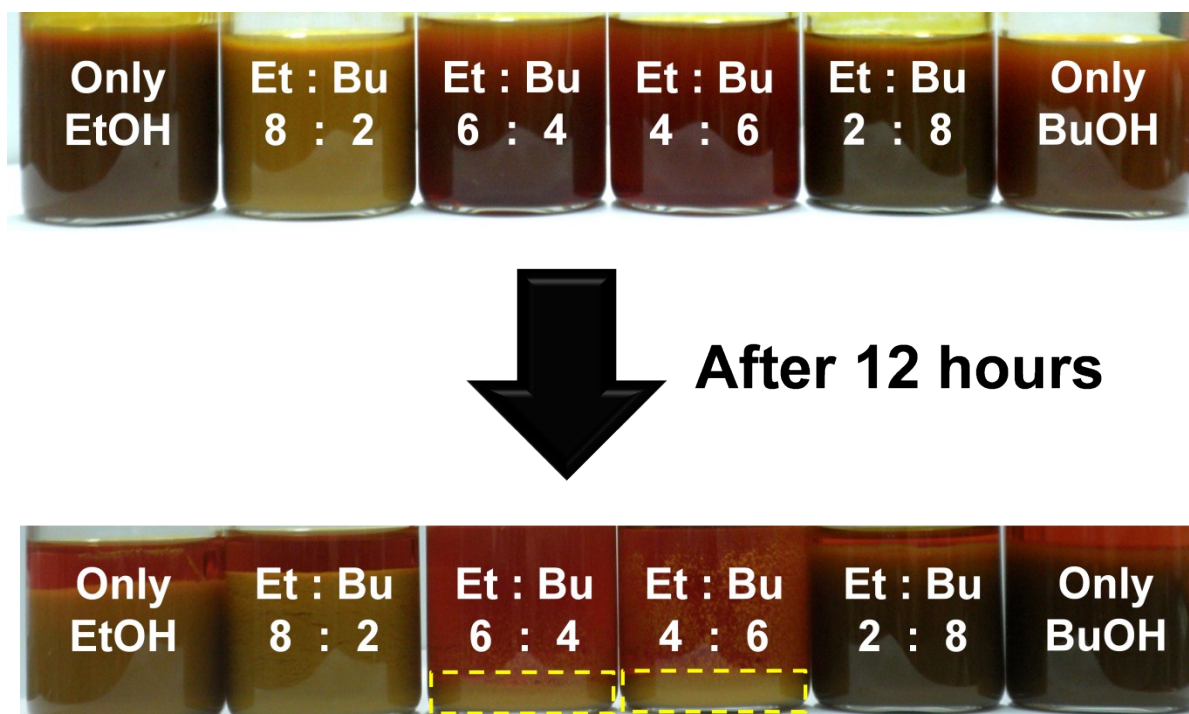


**Figure S1** Photographs of samples prepared at various solvent mixing ratios after 1 h of ultrasonication.

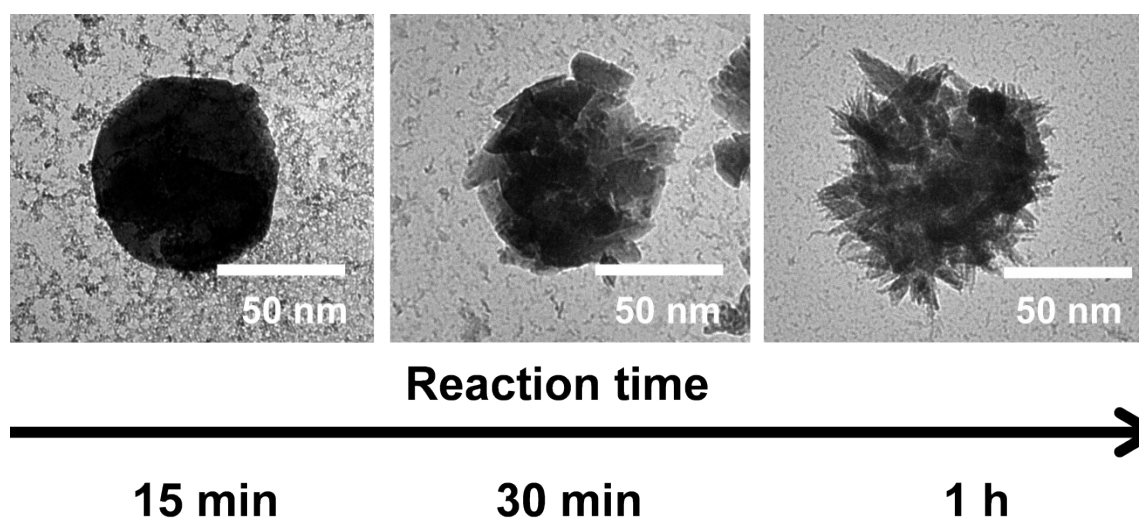


**Figure S2** TEM micrographs of  $\alpha$ -Fe<sub>2</sub>O<sub>3</sub>+PEDOT HNPs as a function of reaction time.

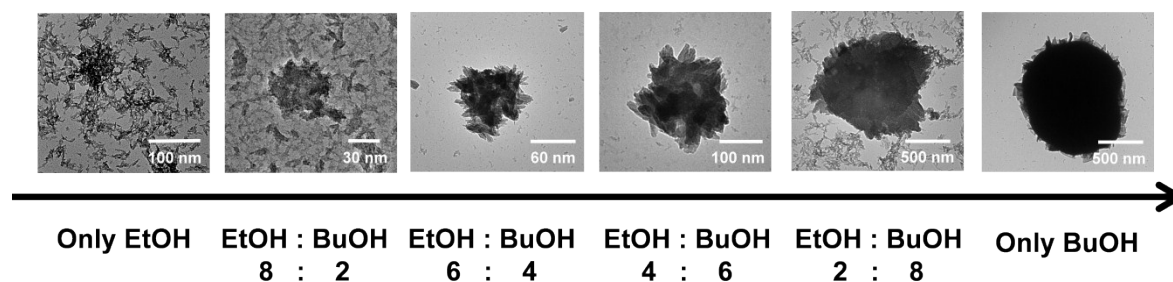


**Figure S3** TEM micrographs of  $\alpha$ -Fe<sub>2</sub>O<sub>3</sub>+PEDOT HNPs as a function of solvent ratio after 1 h of ultrasonication.

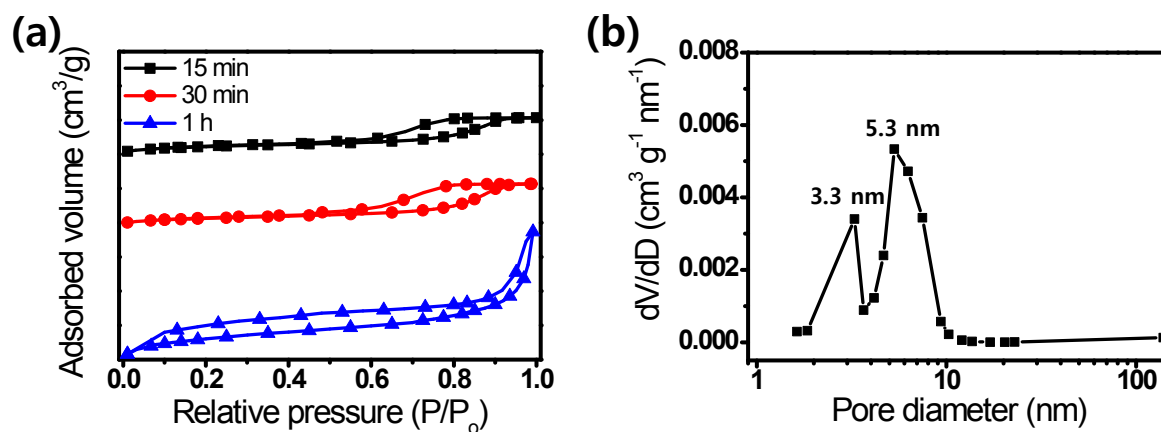


**Figure S4** (a) N<sub>2</sub> adsorption/desorption isotherms of FeO<sub>x</sub> NPs as a function of reaction time (15, 30 min, and 1 h) (b) Barrett–Joyner–Halenda (BJH) pore size distribution curves of FeO<sub>x</sub> NPs.

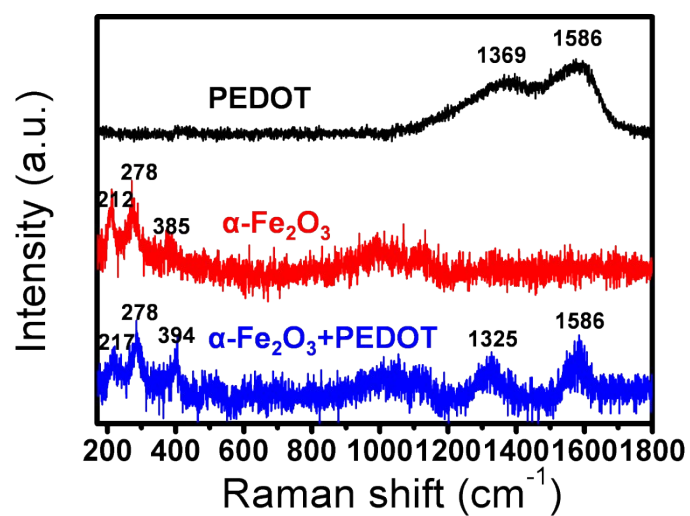


**Figure S5** Raman spectra of PEDOT,  $\alpha$ -Fe<sub>2</sub>O<sub>3</sub>, and  $\alpha$ -Fe<sub>2</sub>O<sub>3</sub>+PEDOT HNPs.

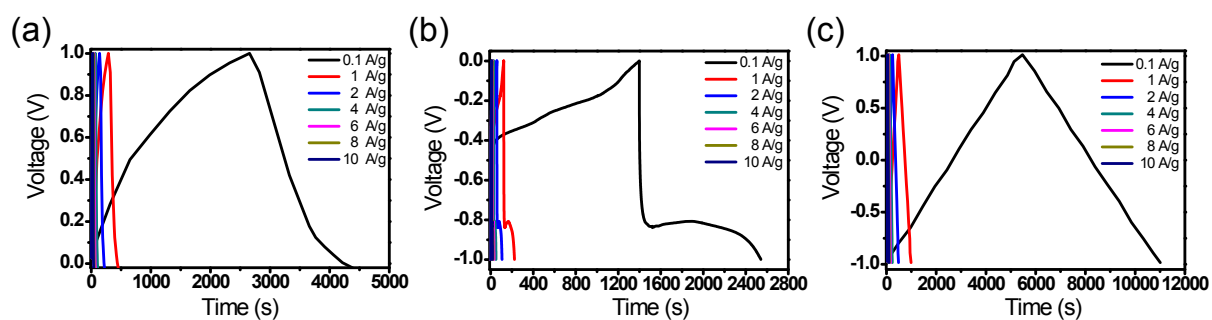


**Figure S6** Galvanostatic charge–discharge curves of (a) PEDOT, (b)  $\alpha$ -Fe<sub>2</sub>O<sub>3</sub>, and (c)  $\alpha$ -Fe<sub>2</sub>O<sub>3</sub>+PEDOT HNPs at various current densities.

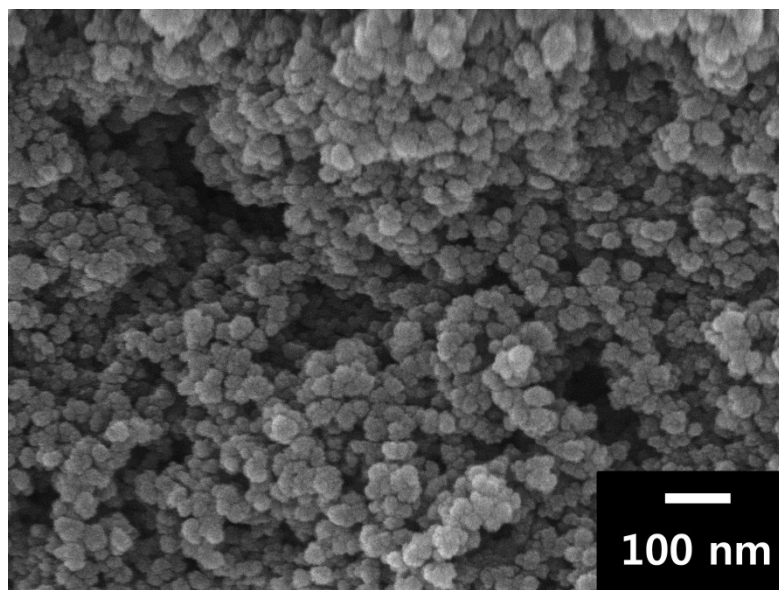


**Figure S7** SEM image of PEDOT NPs.

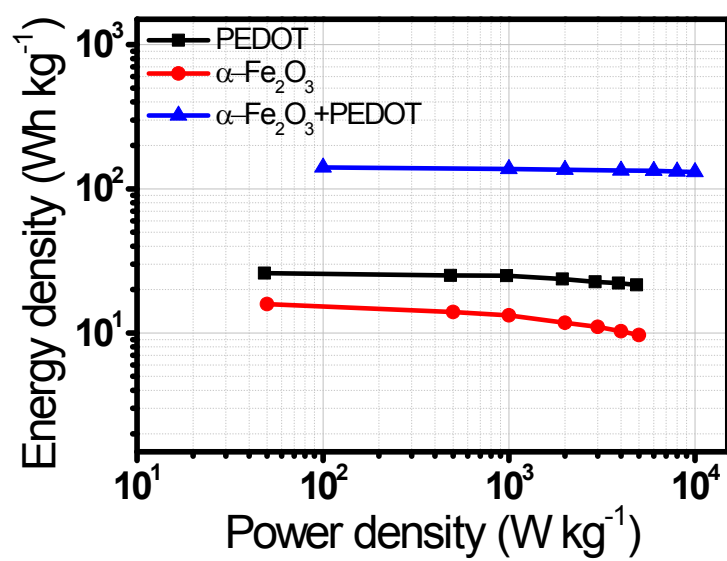


**Figure S8** Ragone plots of PEDOT,  $\alpha$ -Fe<sub>2</sub>O<sub>3</sub>, and  $\alpha$ -Fe<sub>2</sub>O<sub>3</sub>+PEDOT HNPs.

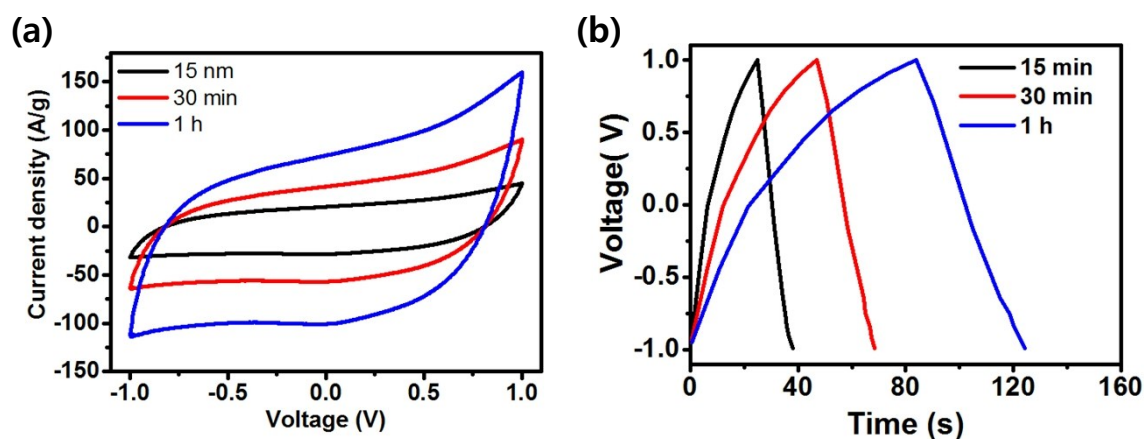


**Figure S9.** (a) Cyclic voltammograms at  $200 \text{ mV s}^{-1}$  scan rate and (b) galvanostatic charge-discharge curves of  $\alpha\text{-Fe}_2\text{O}_3/\text{PEDOT}$  HNPs which made with different reaction times of FeOx through the potential window of  $-1.0$  to  $1.0 \text{ V}$  vs. Ag/AgCl in  $1 \text{ M}$  aqueous  $\text{H}_2\text{SO}_4$ .

We evaluate the cyclic voltammetry curves and galvanostatic charge-discharge curves to investigate the supercapacitive behavior (**Figure S9**). As the reaction time increased, the area under the voltammogram and the discharge time of galvanostatic curve increased, suggesting urchin-like shape FeOx NPs that has higher BET surface area demonstrated better supercapacitive performance than particle shape FeOx NPs that has lower BET surface area.

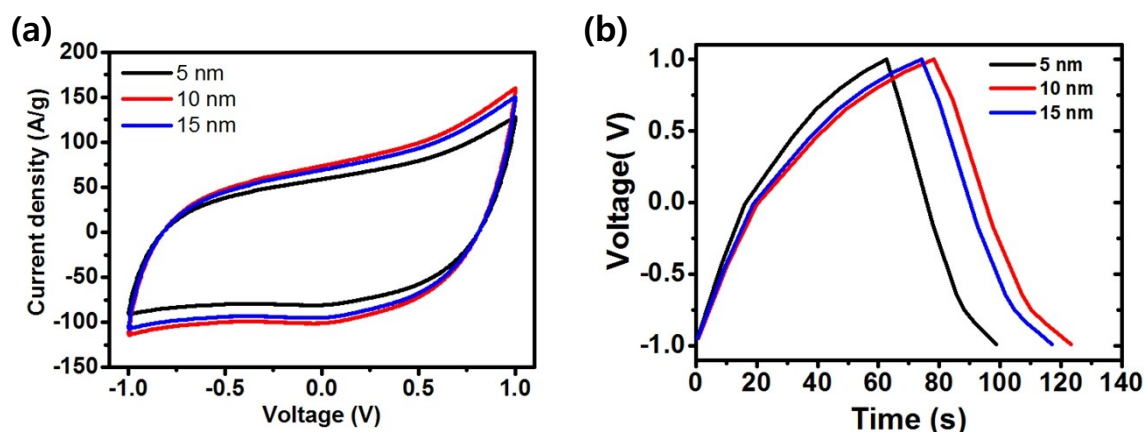


**Figure S10.** Cyclic voltammograms at  $200 \text{ mV s}^{-1}$  scan rate and (b) galvanostatic charge-discharge curves of  $\alpha\text{-Fe}_2\text{O}_3/\text{PEDOT}$  HNPs which made with different shell thickness of PEDOT through the potential window of  $-1.0$  to  $1.0 \text{ V}$  vs.  $\text{Ag}/\text{AgCl}$  in  $1 \text{ M}$  aqueous  $\text{H}_2\text{SO}_4$ .

We demonstrate the supercapacitive performance according to the different PEDOT shell thickness of  $\alpha\text{-Fe}_2\text{O}_3/\text{PEDOT}$  HNPs. As described in **Figure S10**,  $\alpha\text{-Fe}_2\text{O}_3/\text{PEDOT}$  HNPs manifested the best performances at the  $10 \text{ nm}$  of PEDOT thickness. When the thickness of PEDOT increases, the electron conductivity and capacitance increases until  $10 \text{ nm}$ . But if the thickness of shell increases more than  $10 \text{ nm}$ , the aggregation of HNP appears that cause decreases the conductivity and capacitance.<sup>[S1-S2]</sup>

## References

- [S1] X. Xu, Q. Du, B. Peng, Q. Xiong, L. Hong, H. V. Demir, T. K. S. Wong, A. K. K. Kyaw, and X. W. Sun, *Appl. Phys. Lett.* 2014, 105, 113306.
- [S2] S. Han, Y. C. Pu, L. Zheng, J. Z. Zhang, and X. Fang, *J. Mater. Chem. A*, 2015, 3, 22627–22635.